

# **A Thermoresponsive Magnetic Nanoparticle System Using an Antiviral Lectin for HIV Capture and Concentration**

Joseph Phan

A thesis submitted in partial fulfillment of the requirements for the degree of  
Master of Science in Bioengineering

University of Washington  
2015

Committee:  
Kim A. Woodrow  
James J. Lai

Program Authorized to Offer Degree: Bioengineering

©Copyright 2015

Joseph Phan

University of Washington

**ABSTRACT**

A Thermoresponsive Magnetic Nanoparticle System Using an Antiviral Lectin for HIV  
Capture and Concentration

Joseph Phan

Chair of the Supervisory Committee:

Kim A. Woodrow, Assistant Professor

Department of Bioengineering

Rapid tests have been developed as a method to diagnose HIV infection in resource-limited settings. However, several of these assays suffer from reduced sensitivity due to the limited sample volume. One approach to augment the limit of detection is through concentration of the analyte. We used thermoresponsive poly(N-isopropylacrylamide) (pNIPAAm) conjugated to magnetic nanoparticles (MNP) to concentrate HIV from solution. To target HIV for binding and pull-down, we used a novel strategy employing antiviral lectin cyanovirin-N (CVN) rather than commonly used antibodies. We characterize the construction of a thermoresponsive CVN and CVN mutant, and demonstrate successful binding of HIV by the thermoresponsive CVN mutant and roughly 15-fold HIV concentration from a 1 mL sample with greater than 90% efficiency using MNP pNIPAAm. To our knowledge, this is the first evidence of using CVN to bind and concentrate HIV using a thermoresponsive MNP system.

## **ACKNOWLEDGEMENTS**

I would like to express my sincere gratitude to my advisor, Kim Woodrow. Her mentorship and support has truly been invaluable. I would also like to equally thank James Lai. This work was made possible by their support and guidance I also thank: Alex Long for assistance with the CVN mutation to Q62C; Barrett Nehilla for early nanoparticle and conjugate synthesis; Bob Coombs, Reggie Gausman, and Jose Ortega for technical assistance with the RT-PCR work; Cameron Ball, Emily Krogstad, and Renuka Ramanathan for keeping me relatively sane; and the rest of the Woodrow lab for their support, guidance, and friendship. Funding for this work is provided by the University of Washington, the University of Washington Center for AIDS Research, and the National Science Foundation Graduate Research Fellowship Program.

## Table of Contents

<b>1. Introduction .....</b>	<b>1</b>
System design and Conjugation Strategy .....	3
<b>2. Protein expression and Characterization of CVN and Q62C .....</b>	<b>5</b>
2.A. Introduction .....	5
2.B. Materials and Methods.....	6
2.C. Results and Discussion.....	8
2.D. Conclusion .....	11
<b>3. Conjugation of pNIPAAm to CVN and Binding Activity.....</b>	<b>12</b>
3.A. Introduction .....	12
3.B. Materials and methods.....	12
3.C. Results and Discussion.....	15
3.D. Conclusion .....	19
<b>4. Concentration of HIV Using the Thermoresponsive pNIPAAm System .....</b>	<b>20</b>
4.A. Introduction .....	20
4.B. Materials and methods.....	20
4.C. Results and Discussion.....	21
4.D. Conclusion .....	25
<b>5. References.....</b>	<b>27</b>
<b>6. Appendix I.....</b>	<b>31</b>

Figure 1 Gel suggesting successful expression of Q62C/CVN SUMO and cleavage of the SUMO protein. ....	9
Figure 2. MALDI-TOF and Tzm-Bl of CVN and Q62C.....	10
Figure 3. Polyacrylamide gel of pNIPAAm, CVN, and CVN pNIPAAm.....	16
Figure 4. HIV neutralization data of CVN and CVN pNIPAAm in Tzm-Bl cells.. ....	17
Figure 5. MALDI-TOF and polyacrylamide gel of biotinylated Q62C.....	17
Figure 6. Surface plasmon resonance sensograms of interactions of gp120 with biotinylated Q62C .....	18
Figure 7. Capture efficiency and kinetics of temperature-responsive MNPs and SA pNIPAAm.....	23
Figure 8. Percent HIV capture.....	24
Figure 9. HIV enrichment .....	25

# 1. Introduction

Rapid tests have been developed as a method to diagnose diseases in resource-limited settings. These tests are commonly lateral flow assays which are used due to their simplicity and cost. However, several of these assays suffered from reduced sensitivity due to the limited sample volume.<sup>1</sup>

In particular, rapid tests for the monitoring of the treatment of HIV would be useful. Antiretroviral therapy (ART) has seen increasing success in treating HIV affected individuals in sub-Saharan Africa, reaching 56% of those eligible for ART in 2011.<sup>2</sup> For patients on ART, it is important to monitor the status of infection to determine ART efficacy and changes in treatment. As ART resistant HIV strains can develop within days under insufficient quantities of drug, poor monitoring can lead to recurrence of HIV symptoms.<sup>3</sup> The World Health Organization (WHO) advocates the use of viral load to confirm ART failure.<sup>4</sup> Viral load is a measurement of the level of HIV in blood plasma and is typically expressed in units of RNA copies/mL. A value of 1000 RNA copies/mL has been recommended as a threshold for virological failure, as individuals with greater viral loads have predictable antiretroviral mutation patterns, leading to a need to switch to second-line ART.<sup>5-7</sup> While resistance mutations have been detected at viral loads between 50-1000 RNA copies/mL, the highest prevalence of mutations occurred with a viral load between 1000-10000 RNA copies/mL.<sup>8,9</sup> Thus, detecting viral load down to 1000 RNA copies/mL would be beneficial in monitoring ART efficacy.

Real time polymerase chain reaction (RT-PCR) is a commonly used commercial method to determine viral load and can be as sensitive as 40 RNA copies/mL. However, this method requires expensive laboratory equipment and skilled personnel, which is not ideal for resource-limited settings. In order to combat the high costs and complexity of RT-PCR, alternative methods to produce low-cost point-of-care (POC) tests are being developed. Recently, a rapid, low-cost dipstick test has been developed to quantify viral load through detection of viral protein p24.<sup>10</sup> However, this test has a limit of detection of approximately 42500 RNA copies/mL, which is not sufficiently sensitive for monitoring ART effectiveness. These POC tests are largely limited by sample volume, because

they are designed to use around 25  $\mu$ L of sample, thus decreasing the detection limit of total RNA copies. The limitation of low sample volume has created a need for a rapid and simple sample processing strategy for purifying and enriching HIV biomarkers in a form that could be applied to these existing lateral flow tests for increased sensitivity.

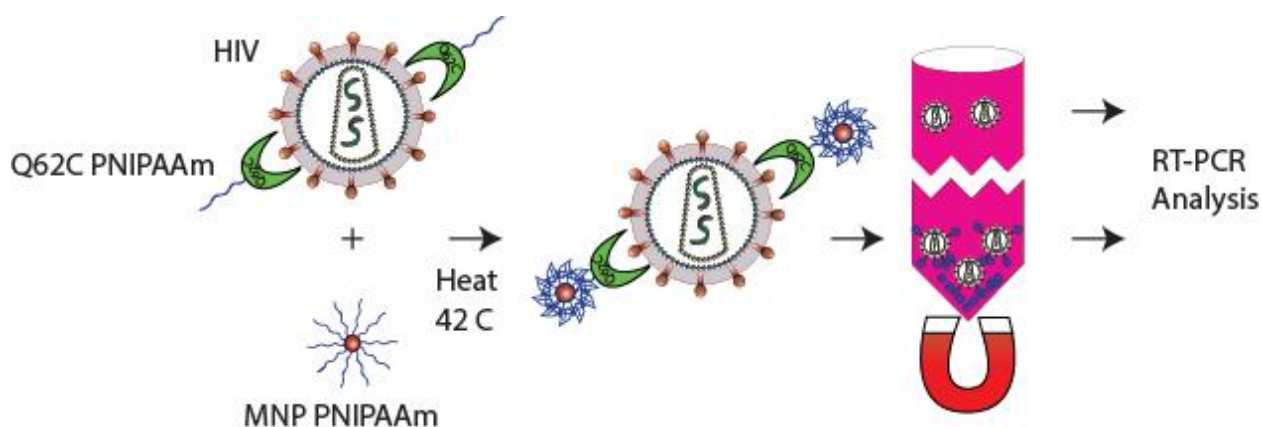
One approach to increase assay sensitivity is to concentrate the target analytes such as virus to a small sample volume appropriate for these low-cost, rapid tests. Kamei *et al.* have developed methodologies to increase the sensitivity of lateral flow assays for viruses and proteins through the use of two-phase systems.<sup>11–13</sup> However, these systems currently require the use of carefully selected PEG-salt ratios, which may limit maximum allowable sample volume. As an alternative, magnetic particles are used commonly to isolate biological molecules.<sup>14</sup> In order to achieve faster and more efficient analyte separation, small iron oxide particles (~5 nm diameter) are coated with poly(N-isopropylacrylamide), pNIPAAm, to overcome challenges of a low magnetophoretic mobility.<sup>15,16</sup> pNIPAAm is a thermally responsive polymer that aggregates in aqueous solution once the temperature is raised above its lower critical solution temperature (LCST) because the polymer undergoes a thermodynamically driven phase transition resulting in a net attraction of the hydrophobic portions of the polymer chain.<sup>17</sup> Magnetic nanoparticles (mNPs) that are coated with pNIPAAm aggregate in aqueous solution above LCST to form micron sized complexes which can be rapidly separated via a modest magnetic field. Temperature-responsive mNPs have been used recently to concentrate malarial antigens via temperature-responsive gold colloids for improving the detection limit of a lateral flow immunoassay.<sup>18,19</sup>

In this thesis, we demonstrate a thermoresponsive magnetic nanoparticle system that uses CVN as an HIV binding molecule to concentrate virus particles and to increase the sensitivity of existing HIV detection strategies. pNIPAAm was conjugated to a CVN mutant through streptavidin interactions. Cyanovirin-N (CVN), is a lectin that can inhibit HIV infection by binding to the gp120 envelope.<sup>20–22</sup> CVN is potent; it prevents HIV fusion from different strains of HIV in the low nanomolar range.<sup>23</sup> CVN is also extraordinarily stable, retaining anti-HIV activity even after multiple freeze-thaw cycles, boiling, and treatment with detergents.<sup>21</sup> CVN is commonly used as an antiviral, but it has not been used as a binding moiety for diagnostic purposes, to our knowledge.



CVN presents an advantage over similar antibodies such as anti-gp120, as it has a high affinity and stability while allowing for more facile and cheaper production in *E. coli*.<sup>24–26</sup> CVN pNIPAAm conjugates were mixed with HIV, and MNP pNIPAAm were used to concentrate the HIV protein complex. Overall, we show the successful construction of CVN and CVN mutant Q62C pNIPAAm conjugates, successful binding of HIV by the thermoresponsive CVN mutant and 15-fold HIV concentration from a 1 mL sample with greater than 90% efficiency using MNP pNIPAAm.

### System design and Conjugation Strategy



**Scheme 1.** Schematic of concentration technique. Q62C PNIPAAm and MNP PNIPAAm are mixed with virus and heated to 42C. The particles are isolated using a magnet and the supernatant collected. The particles are resuspended in PBS and both the particles and supernatant are analyzed using RT-PCR

The strategy for HIV capture and concentration employs a binary reagent system where pNIPAAm, a temperature-responsive polymer, is conjugated to both magnetic nanoparticles (mNPs) and CVN (Scheme 1). The CVN conjugates rapidly diffuse and bind virions via recognition of gp120 on HIV. The solution temperature is then raised above the LCST to aggregate the temperature-responsive reagents with the bound virions via polymer-polymer interactions.<sup>27</sup> The aggregates can be rapidly concentrated by magnetic isolation. The captured virions can be released for downstream processing and analysis by reducing to room temperature to redissolve the aggregates. This binary reagent system where the binding moiety is conjugated to pNIPAAm offers advantages over direct conjugation to the mNPs. As the binding moiety is not attached to a surface, the binding event being diffusion limited is reduced. Moreover, attachment to a surface has been shown to lead to reduced binding efficacy, thought to result from denaturation of the proteins' three-dimensional structure and steric hindrance of binding sites.<sup>28</sup>

Lastly, the concentration of the delivered reagent is independent from the particle concentration, allowing for greater control in driving binding equilibria toward high efficiency.

## 2. Protein expression and Characterization of CVN and Q62C

### 2.A. Introduction

Cyanovirin-N (CVN), a gp120 binding lectin, can inhibit HIV infection by preventing HIV fusion from different HIV strains in the low nanomolar range.<sup>20–23</sup> CVN presents an advantage over similar antibodies such as anti-gp120, as it has a high affinity and stability while allowing for more facile and cheaper production in *E. coli*.<sup>21,24–26</sup> To the best of our knowledge, CVN has not been used as a recognition moiety for diagnostic purposes.

CVN consists of two binding sites that bind selectively to linear oligomannosides containing  $\text{Man}\alpha(1-2)\text{Man}\alpha$ , which are present on gp120.<sup>20</sup> Recent findings suggest that the presence of two carbohydrate binding sites, either through the presence of two intact domains, or by formation of domain swapped dimer form of CVN are necessary for activity.<sup>29,30</sup> Each binding pocket contains 1 accessible lysine, with two other lysines directly adjacent to the binding pockets.<sup>31</sup> Therefore, polymer conjugation via lysine residues can compromise gp120 recognition.

As an alternative strategy to achieve site-specific conjugation, CVN mutant Q62C was expressed along with CVN. Q62C is a mutant of CVN where the glutamine at position 62 is mutated to a cysteine. The mutation has shown minimal decrease in CVN activity, as the residue at position 62 falls outside the CVN binding pockets and is highly solvent accessible.<sup>32</sup> The original four cysteines in CVN present in the form of disulfide bonds, so this mutation enables site-specific conjugation.<sup>33</sup> Therefore, conjugation to the free sulfhydryl on the mutated cysteine may preserve gp120 recognition.

For use in the thermoresponsive magnetic nanoparticle system, the proteins of CVN and Q62C first needed to be expressed. The SUMO construct was used for expression as it has been shown to increase solubility and total protein yield of CVN and other proteins and also allows for purification using a 6x His tag on SUMO.<sup>24,34,35</sup> We successfully show the construction of the CVN-SUMO and Q62C SUMO plasmids, expression of the protein, and functional protein activity to HIV.

## 2.B. Materials and Methods

### Materials

DNA primers were synthesized from Integrated DNA Technologies (Coralville, IA). TZM-bl cells and HIV-1 BaL isolate were obtained from the NIH AIDS Research and Reference Reagent Program, Division of AIDS, NIAID, NIH (<http://www.aidsreagent.org/>).

### Construction of CVN and Q62C sequences.

The CVN sequence was constructed using overlap extension PCR from primers encoding the CVN sequence from Gustafson et al.<sup>33</sup> PCR amplification was performed using the Herculase II DNA Polymerase from Agilent (Santa Clara, CA) using 12.5 pmol of each primer per manufacturer's instructions. The PCR amplified product was purified using a 1% agarose gel in Tris-acetate-EDTA buffer and a Qiaquick kit from Qiagen (Valencia, CA) according to manufacturer's instructions. The PCR product was then inserted into pUC19 plasmid from New England Biolabs (NEB, Ipswich, MA) by cleaving the plasmid with Eco RI and Pst I restriction enzymes (NEB) and ligating using T4 DNA ligase (NEB) according to manufacturer's instructions. The ligation product was isolated using blue-white screening from DH5 $\alpha$  cells (Life Technologies). Plasmid DNA was isolated using a Qiaprep Spin Miniprep kit (Qiagen). The formation of the Q62C mutation, where the 62<sup>nd</sup> glutamine residue was mutated to cysteine, was made using a Quikchange Lightning XL kit from Agilent (Santa Clara, CA).

For protein production, the Q62C sequence was cloned into a pET-SUMO plasmid using the Champion™ pET SUMO expression System (Life Technologies). Forward primer (5' ATG CTT GGT AAA TTC TCC CAG ACC 3') and reverse primer (5' TTA TTC GTA TTT CAG GGT ACC GTC 3') at 50 pmol were mixed with 2.5 ng of Q62C plasmid and PCR amplified using Taq Polymerase (NEB). The insert was ligated into the pET-SUMO plasmid using TA cloning, propagated using One Shot Mach1-T1 Competent cells (Life Technologies), and plasmid purified using a Qiagen miniprep, all according to manufacturer's instructions.

### **Protein Expression and Purification.**

The plasmids encoding Q62C and CVN SUMO were transformed into BL21(DE3) One Shot cells (Life Technologies) for protein expression. Individual colonies from kanamycin lysogeny broth (LB) agar plates were inoculated in a starter culture of 20 mL of LB broth with 50 µg/mL kanamycin and supplemented with 0.5 % (w/v) glucose and 1.6 mM MgSO<sub>4</sub>. The cells were grown overnight at 37 °C at 250 RPM and subsequently transferred to 500 mL of the supplemented LB broth. When the OD<sub>600</sub> reached 0.8, isopropyl-beta-d-thiogalactoyranoside (IPTG) was added to a final concentration of 0.5 mM and the cells were grown at 37 °C for 4.5 hours. Cells were collected by centrifuging at 4400 g (JA-10 Beckman) for 20 minutes. LB broth was decanted, and the cells were frozen at -20 °C for 15 hours.

The cell pellet was resuspended in 20 mL of a lysis buffer (1 mM imidazole, 40 mM NaH<sub>2</sub>PO<sub>4</sub>, 300 mM NaCl, pH 8.0) and 1 mg/mL of lysozyme (Sigma) and 20 µg/mL DNase I (Sigma) were added. The resuspended cells were incubated on ice for 30 minutes and sonicated at 60% power using a 500 watt Branson ultrasonic processor (Sigma). The lysed cells were centrifuged for 30 minutes at 10000 g, and the supernatant was collected for affinity purification.

CVN and Q62C-SUMO was purified using a 5 mL HisTrap FF Ni-NTA column (GE Healthcare, Piscataway, NJ). The column was equilibrated with six column volumes of lysis buffer, and the cell lysate supernatant was applied. The column was washed with a wash buffer (40 mM imidazole, 40 mM NaH<sub>2</sub>PO<sub>4</sub>, 300 mM NaCl, pH 8.0) and Q62C-SUMO was eluted with an elution buffer (250 mM imidazole, 40 mM NaH<sub>2</sub>PO<sub>4</sub>, 300 mM NaCl, pH 8.0). All buffers were flowed through at 5 ml/min. Excess imidazole was removed using 10 kDa molecular weight cutoff Amicon centrifugal filters (Millipore) and buffer exchanged with phosphate buffered saline (PBS).

SUMO was subsequently cleaved using CoolCutter™ SUMO protease (Genecopoeia, Rockville, MD). Uncleaved Q62C SUMO and SUMO were removed by diluting the reaction 1:10 with lysis buffer and applying to an additional HisTrap column. SUMO complexes would bind to the column, while CVN/Q62C would flow through. Protein concentration was determined using a BCA assay (Thermo Scientific).

### **Protein characterization.**

The progress of the protein purification was analyzed using a 4-12% Bis Tris SDS-PAGE gel with MOPS buffer (Invitrogen Life Technologies).. The molecular weight of the proteins was determined using MALDI-TOF (Bruker Autoflex). The proteins were desalted using 7 kDa Zeba columns (Thermo Scientific) and combined in a 1:1 ratio with a 2:1 mixture of Cyano-4-hydroxycinnamic acid and 2,5-dihydroxybenzoic acid using the dried droplet method.

The bioactivity of CVN/Q62C was determined using an HIV inhibition assay. TZM-bL cells were added to black 96-well plates (Corning, Corning, NY) with Dulbecco's Modified Eagle Medium (DMEM) (Gibco Life Technologies) with 10% fetal bovine serum (Hyclone), 1% 100X penicillin/streptomycin (Invitrogen Life Technologies), and 1% 200 mM L-glutamine (Invitrogen Life Technologies) at 50  $\mu$ L/well at a density of 5,000 cells/well. Cells were incubated in 5% CO<sub>2</sub> and 37 °C for 24 h prior to exposure to Q62C. Treatments were added in 50  $\mu$ L volumes. For the HIV-infectious inhibition assay, 100  $\mu$ L of HIV- BaL (240 TCID<sub>50</sub>/well) was added to wells 1 hr after CVN/Q62C treatment. Media was removed from cells after 48 hr post-treatment, and 100  $\mu$ L of phosphate buffered saline (Gibco Life Technologies) and 100  $\mu$ L of Bright-Glo Luciferase reagent (Promega) were added to wells. Infectious activity was quantified by measuring luminescence on a plate reader (Tecan). IC<sub>50</sub> values of drug compounds were estimated using a sigmoidal fit using Prism (Graphpad).

### **2.C. Results and Discussion**

Plasmid construction of CVN was carried out using overlap extension PCR. Afterwards, a single point mutation was made to construct Q62C. The theoretical sequences of CVN and Q62C are shown in Appendix 1. Sequencing of the plasmids after construction showed an exact match to the theoretical sequences, indicating the successful construction of the protein plasmids.

CVN and Q62C were transformed into *E. coli* and expressed fused to a hexahistidine tagged SUMO protein to improve solubility and purification.<sup>24</sup>. CVN-SUMO was purified using a Ni-NTA column, and the SUMO-6xHis was subsequently cleaved using SUMO protease. The protein solution was further purified by using a Ni-NTA

column, where uncleaved CVN-SUMO-6xHis and cleaved SUMO-6xHis were removed. The results of the expression and purification are shown in Figure 1. A protein band corresponding to the theoretical molecular weight of 24 kDa of CVN-SUMO-6xHis is present in the first Ni-NTA purification in lane 1. A band corresponding to the molecular weight of CVN (11 kDa) is present in the 2<sup>nd</sup> Ni-NTA purification in lane 2, albeit with some protein contaminants above 36 kDa. The slight increase in molecular weight of

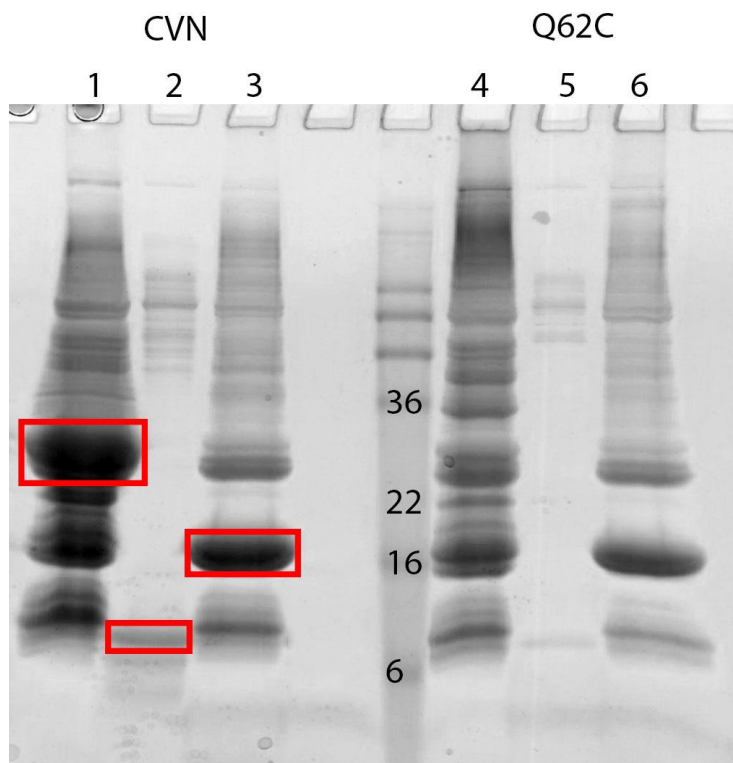


**Figure 1** Gel suggesting successful expression of Q62C/CVN SUMO and cleavage of the SUMO protein. Lane 1 is uncleaved CVN SUMO, lane 2 is cleaved CVN SUMO that has been eluted from a Ni<sup>2+</sup> column, and lane 3 is the cleaved hexahistidine-tagged SUMO. Lanes 4-6 are the same as CVN, except for Q62C.

cleaved SUMO above its expected size of 13 kDa in lane 3 is consistent with earlier reports. Q62C exhibits the same properties as CVN in lanes 4-6. The gel suggests successful expression of CVN/Q62C SUMO and cleavage of SUMO from Q62C/CVN.

Matrix-assisted laser desorption ionization (MALDI), a time-of-flight mass spectrometer was used to confirm the molecular weight of CVN and Q62C (Figure 2A).<sup>24</sup> MALDI analysis of the purified proteins determined a molecular mass of 11117

and 11142 Da for Q62C and CVN, respectively, which is in good agreement with the expected theoretical mass of 11119 and 11144 Da.

Additionally, we also used an *in vitro* anti-HIV TZM-bl inhibition assay to verify that Q62C and CVN recognize HIV virions. CVN binds to linear oligomannosides containing Man $\alpha$ (1-2)Man $\alpha$  glycans on the gp120 envelope protein of HIV results in virus neutralization,<sup>20</sup> which can be measured *in vitro* using a reporter cell assay. The purified Q62C protein exhibited potent antiviral activity and had a measured IC<sub>50</sub> value of 4.2 nM (Figure 2B), the Q62C concentration required to inhibit HIV infection by 50%.

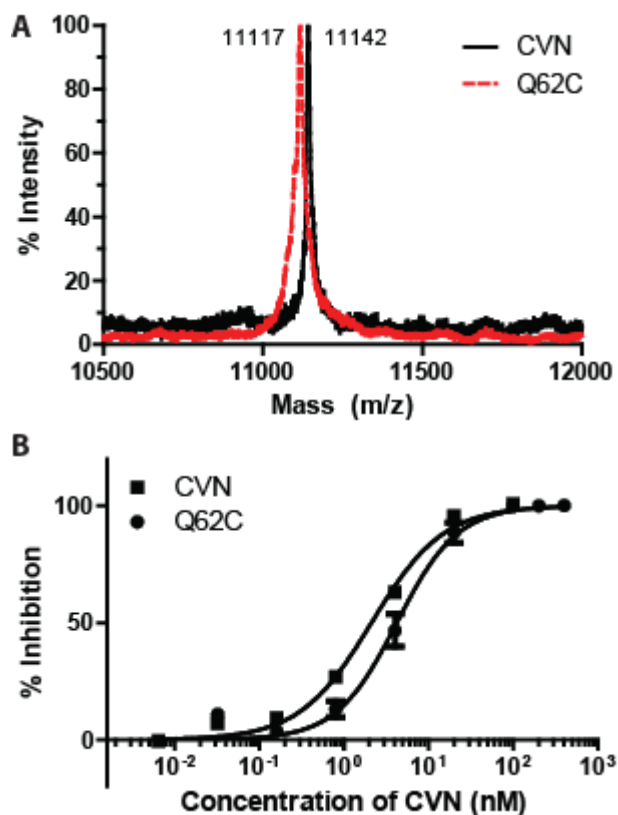


**Figure 2.** CVN and Q62C are expressed and functional. (A) MALDI-TOF spectrum of CVN and Q62C. The molecular weight of Q62C confirms the mutation. (B) HIV neutralization data of Q62C and CVN in Tzm-BI cells. IC<sub>50</sub> values of 4.2 and 2.1 nM for Q62C and CVN, respectively, indicate binding to HIV.

Compared to the IC<sub>50</sub> value of 2.1 nM for wild type CVN, the inhibition of HIV infection via Q62C is less efficient, in accordance with previously published data from others.<sup>32</sup> These IC<sub>50</sub> values show that both proteins inhibit HIV infection at low nanomolar



concentrations and indicates effective HIV binding. Collectively, the TZM-bl and SPR data in conjunction with the molecular mass characterization indicates successful expression of Q62C and CVN.

## **2.D. Conclusion**

We demonstrated the successful expression and activity of CVN and Q62C. As shown by gel, the SUMO portion of the protein was cleaved by the protease. The molecular weight of both proteins were confirmed by MALDI-TOF and shown to be functional against HIV using the TZM-bl assay. With functional proteins successfully expressed, we proceeded to conjugate thermoresponsive polymer pNIPAAm and test the binding activity of the conjugates.

### 3. Conjugation of pNIPAAm to CVN and Binding Activity

#### 3.A. Introduction

With Q62C and CVN successfully expressed, we proceeded to conjugate thermoresponsive polymer pNIPAAm to the proteins to use with the thermoresponsive magnetic nanoparticle system. We first conjugated pNIPAAm to CVN through the primary amines and tested its activity through antiviral activity. We then proceeded to construct the Q62C pNIPAAm through streptavidin biotin interactions. We successfully show the conjugation of pNIPAAm to the proteins and retention of activity in the CVN mutant, Q62C.

#### 3.B. Materials and methods

##### Materials.

4-Cyano-4-(ethylsulfanylthiocarbonyl) sulfanylpentanoic acid (ECT) was synthesized as previously reported.<sup>36</sup> 2-(Dodecylsulfanylthiocarbonylsulfanyl)-2-methylpropionic acid (DMP) was a gift from Noveon, 4,4'-Azobis(4-cyanopentanoic acid) (V-501, ≥75%), N-isopropylacrylamide (NIPAAm, 97%), 2,2'-Azobisisobutyronitrile (AIBN), tetraglyme (99%), Iron(0) pentacarbonyl (99.99%), dichloromethane, dimethyl sulfoxide, THF, and 1,4-dioxane, were obtained from Sigma. AIBN and NIPAAm were recrystallized from ethanol and hexane, respectively, but all other chemicals were used as received without further purification. TZM-bl cells and HIV-1 BaL isolate were obtained from the NIH AIDS Research and Reference Reagent Program, Division of AIDS, NIAID, NIH (<http://www.aidsreagent.org/>). Biotin-PEG2-MAL was obtained from Life Technologies (Grand Island, NY).

##### Synthesis of pNIPAAm.

pNIPAAm was synthesized by reversible addition fragmentation chain transfer (RAFT) polymerization. Specifically for protein conjugation, a homo-pNIPAAm polymer with target molecular weight of 36 kDa was polymerized by dissolving 4.97 g of NIPAAm (43.9 mmol), 32.6 mg of ECT (0.120 mmol), 3.5 mg of V-501 (0.012 mmol) into 12.5 g of

1,4-Dioxane in a round bottom flask. The molar ratio of monomer to chain transfer agent to initiator was 365/1/0.01. The flask was purged for 20 minutes with nitrogen, heated at 70 °C for 4 hours, and precipitated into pentane. The product was dried in vacuum overnight. A 5 kDa homo-pNIPAAm polymer for use with MNP was polymerized by dissolving 2 g (17.7 mmol) of NIPAAm, 143.3 mg (0.4 mmol) of DMP, 6.6 mg of AIBN (40.5 μmol) of AIBN into 4 g of 1,4-Dioxane in a round bottom flask. The molar ratio of monomer to chain transfer agent to initiator was 45/1/0.1. Purification and precipitation carried out identically to 36 kDa pNIPAAm.

PNIPAAm was characterized using GPC performed on an Agilent 1200 series liquid chromatography system, equipped with TSKgel alpha 3000 and TSKgel alpha 4000 columns (TOSOH biosciences). The mobile phase was LiBr (0.01 M) in HPLC grade DMF at a flow rate of 1 mL min<sup>-1</sup>. MALS data were obtained on a miniDAWN TREOS (Wyatt Technologies Corp.) with 658 nm laser source, and three detectors at 45.8°, 90.0°, and 134.2°. The instrument calibration constant was 4.7460 × 10<sup>-5</sup> V<sup>-1</sup> cm<sup>-1</sup>. Refractive index was measured using an Optilab Rex detector (Wyatt Technologies Corp.). The  $dn/dc$  value for the PNIPAAm was determined under the assumption of 100% mass recovery by injecting polymer samples at known concentrations into the RI detector postcolumn. The  $dn/dc$  value was then calculated using linear regression with the Astra 5.3.4.14 data analysis software package (Wyatt Technologies Corp.).

### **Synthesis of pNIPAAm magnetic nanoparticles (MNP pNIPAAm).**

900 mg of 5 kDa pNIPAAm was dissolved in 50 mL of tetraglyme by heating at 100 °C for 10-15 minutes in a round bottom flask. 200 μL of Iron pentacarbonyl (Fe(CO)<sub>5</sub>) was added to the flask and the temperature was raised to 190 °C for 6 hours. The mixture was cooled for 15 minutes, the MNP were precipitated in pentane and re-dissolved in THF. The precipitation was repeated 3 times. Extra solvent was removed using a vacuum and unreacted polymer removed via ultrafiltration using a stir cell (Millipore). The product was then lyophilized.

### **Formation of protein-polymer conjugates.**

Streptavidin was conjugated to pNIPAAm using NHS chemistry. Streptavidin (SA) was bought from Thermo Scientific. pNIPAAm was dissolved in dichloromethane and N-Hydroxysuccinimide and dicyclohexylcarbodiimide was added at a 10 times molar concentration to pNIPAAm. The flask was purged for 10 minutes with nitrogen and stirred overnight at 25 °C. The polymer solution was filtered, precipitated into hexane, and dried in vacuum. Streptavidin was buffer exchanged with a sodium bicarbonate buffer, pH 9.5 using a 7 kDa Zeba column. NHS pNIPAAm dissolved in anhydrous dimethyl sulfoxide was added to Streptavidin at a 100:1 molar ratio and at a 1:9 volume ratio and left overnight at 4 °C. Unreacted streptavidin was removed by using thermal precipitation. In this procedure, the protein-polymer solution was heated at 40 °C and centrifuged at 21000 g for 10 minutes. The supernatant was removed, and the polymer pellet was resuspended in PBS. This procedure was repeated 3x. Excess pNIPAAm was removed using a 10 kDa molecular weight cutoff Amicon filter (EMD Millipore). The number of biotin binding sites of SA pNIPAAm was determined using a HABA kit (Thermo Scientific).

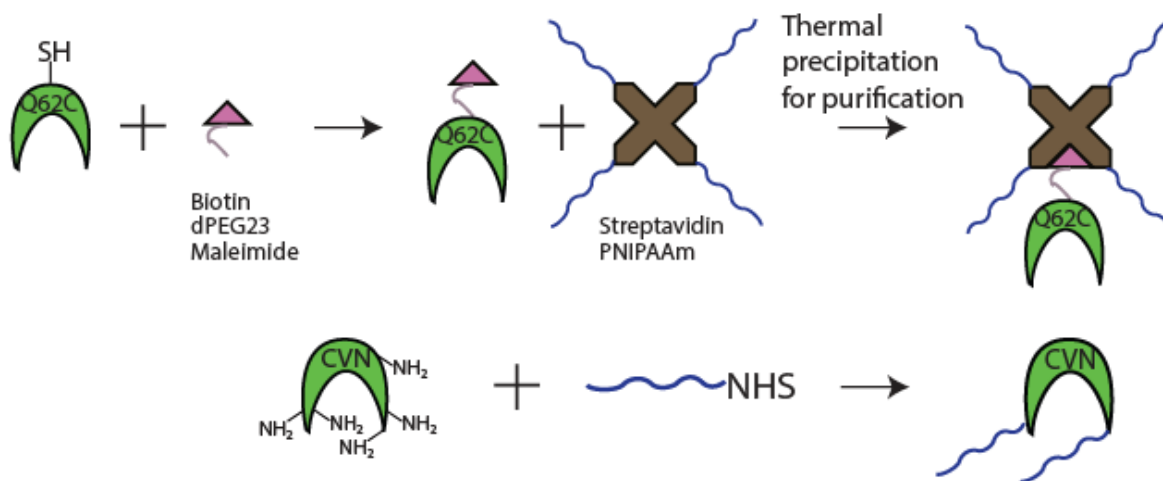
Q62C was first biotinylated through the free cysteine residue using biotin-PEG2-MAL. Dithiothreitol (DTT, Bio-Rad, Hercules, CA) was added to Q62C and incubated for 2 hours at 25 °C. The DTT was removed and buffer exchanged with a sodium phosphate buffer (0.1 M sodium phosphate, 1 mM Ethylenediaminetetraacetic acid, pH 6.5) using a 7 kDa Zeba column. Biotin-PEG2-MAL was dissolved in DMSO and reacted for 2 hours at 25 °C. Excess biotin-PEG2-MAL was removed using a PD-10 column (GE Healthcare). Unbiotinylated Q62C was removed using SoftLink™ Soft Release Avidin Resin (Promega) according to manufacturer's instructions using a Tris buffer (50 mM Tris, 150 mM NaCl, pH 8.0) as the equilibration buffer. Excess biotin from the avidin purification was removed using a 7 kDa Zeba column.

### **Measuring binding affinity of biotinylated Q62C.**

The binding ability of biotinylated Q62C was determined using surface plasmon resonance (SPR) on a Biacore T200 (GE Healthcare). Biotinylated Q62C was immobilized to a sensor CAP chip (GE Healthcare) through streptavidin interactions to a RU of 10. Binding experiments were performed in 10 mM HEPES–150 mM NaCl–3 mM EDTA–0.05% surfactant P20, pH 7.4 (HBS-EP) at 25 °C. A reference flow cell was used

to account for nonspecific binding. Gp120 HIV-1 IIB produced from baculovirus (Immunodiagnosics, Woburn, MA) was spiked with 0.1 mg/mL sheared salmon sperm DNA (Life technologies) to reduce non-specific binding and injected at 30  $\mu\text{L}/\text{min}$  for 2 minutes, with the dissociation being monitored for 5 minutes while washing with buffer. The surface was regenerated using a 3:1 8 M guanidine-HCl, 1 M NaOH.

### 3.C. Results and Discussion



**Scheme 2.** Conjugation strategy for CVN and Q62C PNIPAAm. CVN pNIPAAm was formed using NHS chemistry. Q62C PNIPAAm was formed using site-specific maleimide chemistry to attach biotin to a streptavidin PNIPAAm.

#### Temperature-responsive protein conjugates.

Thermoresponsive CVN was constructed by conjugating CVN to PNIPAAm through two strategies (Scheme 2). For wild type CVN, a RAFT-polymerized carboxyl-terminated PNIPAAm that was activated with DCC/NHS was reacted with primary amines on CVN. As the binding pockets of CVN contain solvent accessible lysines, the affinity of CVN could be diminished using this DCC/NHS technique. In order to achieve site-specific conjugation, maleimide chemistry was used to conjugate to the free sulfhydryl on the cysteine on Q62C. We hypothesized that conjugation to the free sulfhydryl on the mutated cysteine would retain a greater binding activity than the DCC/NHS method.

Verification of successful conjugation of CVN to PNIPAAm was performed by polyacrylamide gel. 40 kDa PNIPAAm was used for CVN conjugation, as polymers of

that size have exhibited thermal activity.<sup>37</sup> With successful conjugation of PNIPAAm, the CVN band at 11kDa should shift to a molecular weight greater than 51 kDa. The conjugate showed disappearance of the CVN band and the presence of a smear pattern greater than 250 kDa, while PNIPAAm alone did not (Figure 3). This suggests that each CVN is conjugated to multiple molecules of PNIPAAm. MALDI was attempted to further characterize the conjugate, but CVN PNIPAAm did not ionize, leading to a non-detectable signal (data not shown).

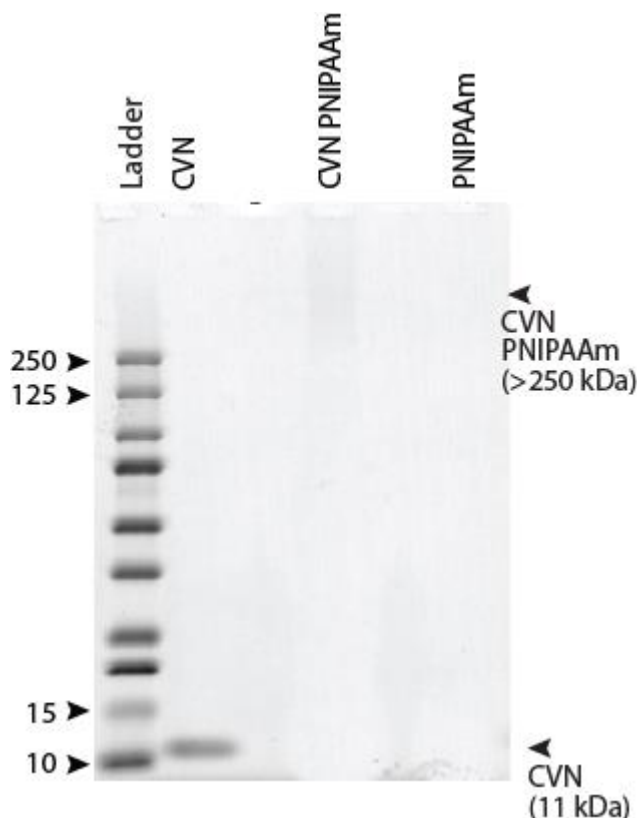


**Figure 3.** CVN successfully conjugated to pNIPAAm. Polyacrylamide gel of pNIPAAm, CVN, and CVN pNIPAAm. Diffuse band greater than 250 kDa in CVN pNIPAAm lane indicative of successful conjugation.

We used an *in vitro* anti-HIV TZM-bl inhibition assay to initially test whether CVN pNIPAAm recognized HIV virions. The results are shown in Figure 4. Although there were insufficient points to calculate an exact value for the IC<sub>50</sub>, the 40% inhibition at 100 nM CVN pNIPAAm indicates that the IC<sub>50</sub> value has increased approximately two orders of magnitude. This drastic reduction in efficacy is likely due to the pNIPAAm conjugated to the lysines within the binding pocket of CVN. Due to this large decrease in efficacy of

CVN pNIPAAm, we decided to further pursue the formation of thermoresponsive CVN through the use of CVN mutant Q62C in order to achieve site-specific conjugation.

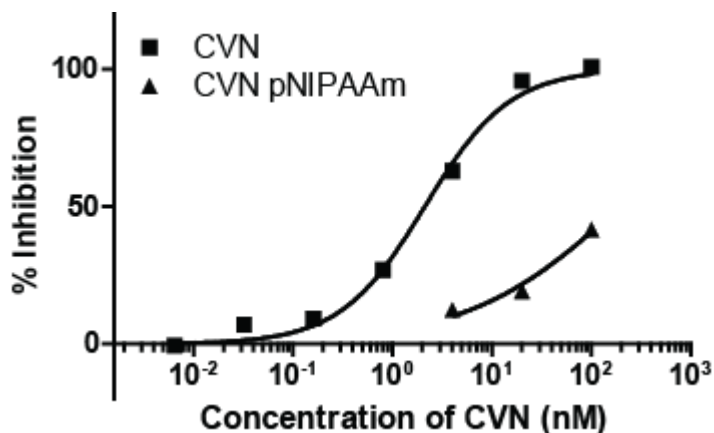


**Figure 4.** HIV neutralization data of CVN and CVN pNIPAAm in Tzm-BI cells. The IC<sub>50</sub> value for CVN pNIPAAm is at least two orders of magnitude higher than CVN.

Temperature responsive Q62C conjugate was constructed through streptavidin-biotin interactions (Scheme 2). Q62C was biotinylated by reacting the cysteine at position 62 with a maleimide-PEG-biotin. Streptavidin-pNIPAAm (SA-pNIPAAm) was synthesized by grafting streptavidin with pNIPAAm, containing a chain-end NHS ester, via covalent linkage. The biotinylated Q62C was then complexed with SA-pNIPAAm to form the final temperature-responsive conjugate, Q62C-pNIPAAm.

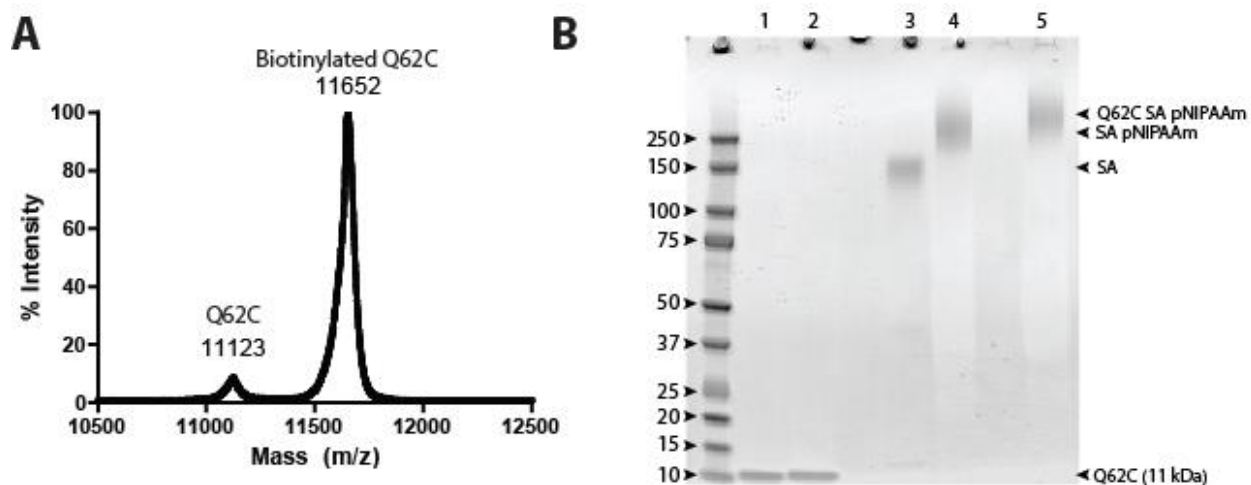


**Figure 5.** Q62C was conjugated to PEG2-biotin. (A) MALDI-TOF spectra of Q62C biotin PEG2 conjugate. A 1450 Da increase in mass is indicative of conjugation to biotin PEG2. (B) Polyacrylamide gel of steps of conjugation process. Lane 1 is Q62C, lane 2 is biotinylated Q62C, lane 3 is streptavidin, lane 4 is streptavidin pNIPAAm, and lane 5 is biotinylated Q62C mixed with streptavidin pNIPAAm. The shift of the smear pattern of Q62C SA pNIPAAm over SA pNIPAAm and biotinylated Q62C confirm complexation of biotinylated Q62C with SA pNIPAAm.

The Q62C biotinylation was carried out by following the vendor's protocol (Thermo Scientific). The biotinylated Q62C was characterized using MALDI, following purification using a monomeric avidin column. The MALDI analysis shows a peak at 11123 Da for Q62C and 11652 Da for the biotinylated Q62C (Figure 5A). The biotinylated Q62C exhibits higher molecular weight because of the conjugation of maleimide-PEG-biotin, which is 525 Da. The presence of the Q62C peak indicates the presence of less than 10% unconjugated protein.

Surface plasmon resonance (SPR) was used to confirm that biotinylated Q62C recognizes gp120. As recognition of binding to gp120 is a more direct measure of binding efficacy in comparison to the TZM-bl assay, the TZM-bl assay was not repeated for biotinylated Q62C. Biotinylated Q62C was immobilized on the surface of a BIAcore CAP chip coated with streptavidin. Upon injection of gp120 (strain IIIB) to the sensor chip, we measured a dissociation constant of 0.60 nM (Fig 6 and Table 1). This value is comparable to the previously measured 1.9 nM dissociation constant for wild type CVN for gp120 (strain 89.6).<sup>22</sup> The retention of a low dissociation constant after biotinylation

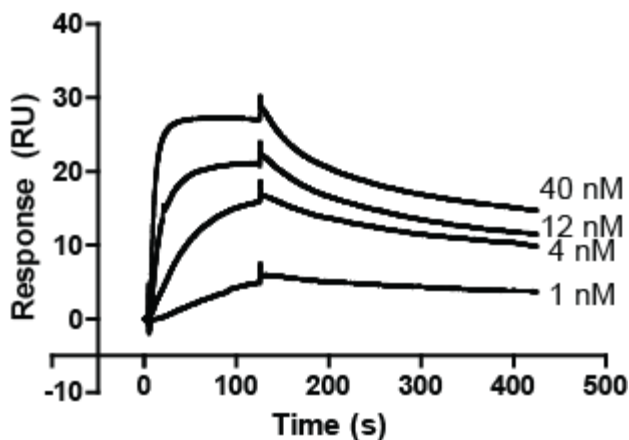


**Figure 6.** Biotinylated Q62C retains binding activity to gp120. Surface plasmon resonance sensograms of interactions of gp120 with biotinylated Q62C on a CAP chip. Q62C capture level was kept at 10 RU.

is indicative of binding activity to gp120.



	$k_{on}$	$k_{off}$	$K_d$
	$M^{-1}s^{-1}$	$s^{-1}$	nM
Biotinylated Q62C	3.55e6	2.14e-3	0.60

**Table 1.** SPR binding parameters determined for biotinylated Q62C binding with HIV-BaL.

The biotinylated Q62C was complexed with SA-pNIPAAm to form Q62C-pNIPAAm. SA-pNIPAAm was synthesized and purified by following our previous publications with minor modification.<sup>37</sup> Q62C-pNIPAAm was formed through biotin-streptavidin interactions between biotinylated Q62C and SA-pNIPAAm, forming a thermoresponsive protein construct. The resulting Q62C-pNIPAAm was characterized using polyacrylamide gel (Figure 5B) to confirm the complexation. SA-pNIPAAm (Lane 3) shows a smear pattern shifted toward a higher molecular weight than native streptavidin (Lane 4), which confirmed the conjugation of pNIPAAm to SA. Q62C-pNIPAAm (Lane 5) has a smear pattern shifted toward higher molecular weight than Q62C and biotinylated Q62C (Lane 1 and Lane 2) and SA-pNIPAAm (Lane 3), confirming complexation of biotinylated Q62C and SA-pNIPAAm, forming Q62C-pNIPAAm. These results confirm that Q62C-pNIPAAm was successfully formed and purified.

### 3.D. Conclusion

We demonstrated the successful construction of CVN and Q62C pNIPAAm. As shown by gel, multiple units of pNIPAAm were conjugated to CVN. However, the CVN pNIPAAm showed reduced activity in the TZM-bl assay, so we moved forward with Q62C. Successful biotinylation of Q62C was confirmed and retention of activity shown using SPR. With biotinylated Q62C showing binding activity to gp120, we proceeded to test the binding activity of Q62C pNIPAAm within the context of the thermoresponsive magnetic nanoparticle system.

## **4. Concentration of HIV Using the Thermoresponsive pNIPAAm System**

### **4.A. Introduction**

With Q62C pNIPAAm successfully constructed, we proceeded to combine it with temperature-responsive mNPs and HIV to determine the concentration efficiency. We first optimized the concentration of magnetic nanoparticles and pulldown time to maximize thermoresponsive protein capture. We then proceeded to combine the virus, particles and Q62C pNIPAAm together. We successfully show the capture and concentration of HIV using the thermoresponsive mNP system.

### **4.B. Materials and methods**

#### **Measuring percent and speed of pulldown of SA pNIPAAm using MNP.**

For time based studies, 500 nM SA pNIPAAm solutions were mixed with 0.5 mg/mL MNP pNIPAAm in 250  $\mu$ L of PBS. The samples were heated to 42  $^{\circ}$ C for 5 minutes using a heat block, and were subsequently transferred to a magnet in 42  $^{\circ}$ C incubator for 0.5-15 minutes. For both studies, the supernatant was removed and the amount of streptavidin was quantified using a fluorescence quenching assay involving streptavidin and biotin-4-fluorescein (B4F, Life Technologies).<sup>38</sup> Briefly, 8 nM B4F exhibits a linear relationship between fluorescence signal and streptavidin concentrations less than 2 nM. The supernatant was diluted in PBS to be within the estimated 2 nM range with 0.1 mg/mL bovine serum albumin (BSA) and added to B4F in PBS with 0.1 mg/mL BSA at 8 nM and left at 25  $^{\circ}$ C for 30 minutes. Fluorescence emission at 525 nm (excitation 490 nm) was measured using a plate reader (Tecan M200). Lower concentrations of streptavidin correlated to higher fluorescence signal.

#### **Virus Concentration.**

For the initial virus pulldown study, the virus was diluted to  $2 \times 10^6$  virus copies/mL in PBS and mixed with biotinylated Q62C for 10 minutes at 25  $^{\circ}$ C at a total volume of 100

μL. SA pNIPAAm was added in a fourfold excess at a 1:1 ratio with the biotinylated Q62C and mixed for 5 minutes. MNP pNIPAAm was added at 0.5 mg/mL and mixed for 5 minutes, and the conjugate-virus-MNP solution was heated to 42 °C for 5 minutes. The solutions were moved to a magnetic rack at 42 °C for 5 minutes. The supernatant was extracted from the MNP pellet, and the MNP were resuspended in 100 μL PBS.

The supernatant and pellet were analyzed using RT-PCR. The viral RNA was extracted using NucliSens® miniMAG®(Biomerieux, Marcy l'Etoile, France) according to manufacturer's instructions. Armored RNA HIV-1 standards subtype B in TSM buffer standards were specially ordered from Ambion.<sup>39</sup> Primers used were HXB2-Gag-F (5' CAA GCA GCC ATG CAA ATG TT 3') and SK431 (5' TGC TAT GTC ACT TCC CCT TGG TTC TCT 3') from Invitrogen. The forward probe consisted of an HXB2 oligonucleotide with a 5'-FAM reporter dye (6-carboxyfluorescein) and a 3'-Tamra quencher dye (6-carboxy-N,N,N',N'-tetramethylrhodamine) with sequence (5' -6-FAM-AAA GAG ACC ATC AAT GAG GAA GCT GCA GAA 3'). The reverse probe consisted of an AR-8 oligonucleotide with a 5' FAM reporter dye and a 3' minor groove binder/non fluorescent quencher (5'-6-FAM-CTA TCC CAT TCT GC 3-MGBNFQ). Both probes were from Applied Biosystems Life Technologies. PCR enzymes were from AgPath-ID™ one-step RT-PCR kit (Ambion Life Technologies). RT-PCR was run according to manufacturer's instructions on an ABI Prism 7900 sequence detection system.

For enrichment studies, the virus was diluted to 2500 virus copies/mL in a total volume of 100, 200, 500, and 1000 μL. The volumes were split evenly among microcentrifuge tubes to fit in the magnetic rack. The rest of the pulldown procedure remained the same as above.

#### **4.C. Results and Discussion**

**Separation via temperature-responsive binary reagent system.** The binary reagent system enables the magnetic separation of HIV virions via the combination of temperature-responsive mNPs and Q62C-pNIPAAm. We first optimized the mNP separation by varying mNP concentration. We optimized the reagent concentrations and time for pNIPAAm conjugated proteins to undergo thermal precipitation and magnetic separation using pNIPAAm grafted MNPs. In order to ensure the system maximum efficiency of virus enrichment in later steps, we first optimized the

concentration of MNP pNIPAAm to undergo magnetic separation. The pulldown efficiency of the MNP pNIPAAm was greater than 90% between ranges 0.5-2 mg/mL (Figure 7A). At concentrations significantly above 2 mg/mL, the increased viscosity of the solution impeded MNP capture.

We varied the time for magnetic isolation to optimize capture efficiency of the SA pNIPAAm. As a potential upstream concentration component to a rapid diagnostic test, the time to completion could affect its adoption rate in a resource-limited setting. We tested capture of 500 nM SA-pNIPAAm, as the maximum concentration of Q62C needed to capture virus should not exceed this amount. We observed that SA-pNIPAAm capture efficiency was >90% after only 30 seconds, and reached 98% capture efficiency after 10 minutes (Figure 7B). Combined with the 5 minute heating time, the SA-pNIPAAm target can be captured with greater than 90% efficiency in a total of 5.5 minutes using our binary reagent system. This speed is comparable to existing HIV separation technologies, such as the Miltenyi  $\mu$ MACS HIV isolation kits, but offers the benefit of not needing a special separation column, which could reduce complexity and cost. The quick capture time of this MNP pNIPAAm system makes it amenable for use with rapid diagnostic tests.

#### **HIV isolation and concentration.**

Immunoaffinity approaches that separate analytes rapidly with high efficiency can potentially shorten the downstream assay time and enhance the sensitivity. The binary reagent system enables the magnetic separation of HIV virions via the combination of temperature-responsive mNPs, pNIPAAm-SA, and biotinylated Q62C (Scheme 1).

For assessing HIV separation via the binary reagent system, a series of samples containing  $5 \times 10^5$  virions/mL (100 $\mu$ l), pNIPAAm-SA 31  $\mu$ g/ml, and mNPs 0.5 mg/mL with varying ratios of biotinylated Q62C-to-HIV virion ranging from  $7.5 \times 10^5$  to  $1.8 \times 10^{11}$  were prepared using PBS. The amounts of mNP and pNIPAAm-SA determined through the optimization of the separation kinetics and efficiency (Figure 7). After 20 minutes incubation at room temperature, the samples were heated to 42°C for 5 minutes to aggregate mNPs, pNIPAAm-SA, biotinylated Q62C, and the bound virions. Then, a magnetic field was applied to heated solutions for 5 minutes to capture the aggregates. The viral loads in the supernatant and aggregate after the separation ( $C_{post-separation}$ ) was

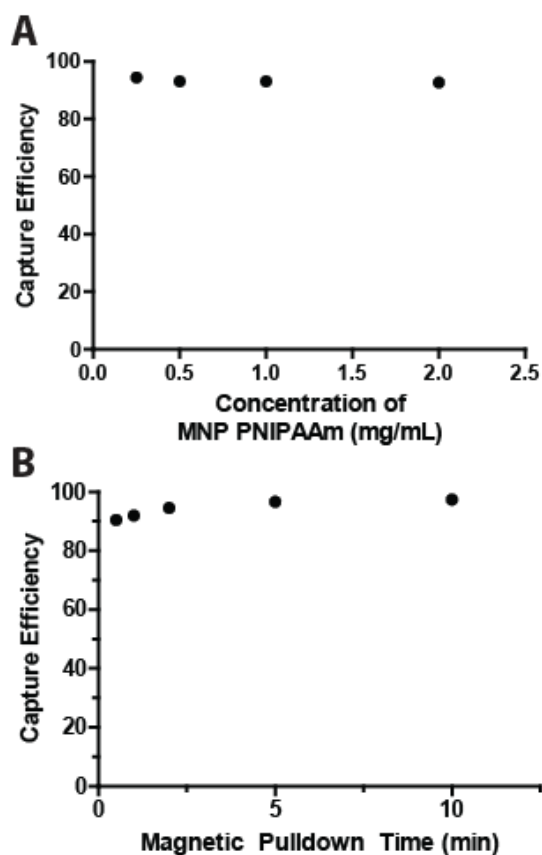


**Figure 7.** (A) Temperature-responsive MNPs can be captured with greater than 90% efficiency at 0.5 mg/mL MNP. Capture efficiency calculated by subtracting absorbance at 500 nm after pulldown from the initial absorbance and dividing by initial absorbance. (B) Temperature-responsive MNPs can pull down SA PNIPAAm with greater than 90% efficiency after 30 seconds. Capture efficiency calculated by dividing concentration of SA PNIPAAm in supernatant by initial concentration.

determined by RT-PCR. HIV separation efficiency ( $\epsilon$ ) was estimated by normalizing the difference between the initial viral load ( $C_i$ ) before the separation and  $C_{post-separation}$  to  $C_i$  (Equation 1).

$$\epsilon = \frac{C_i - C_{post-separation}}{C_i} \times 100\% \quad (1)$$

We achieved a maximum viral capture of 97% when the separation utilized 60 nM PNIPAAm-Q62C (Figure 8). Moreover, we observed a concentration dependent increase in virus separation efficiency as we increased the PNIPAAm-Q62C

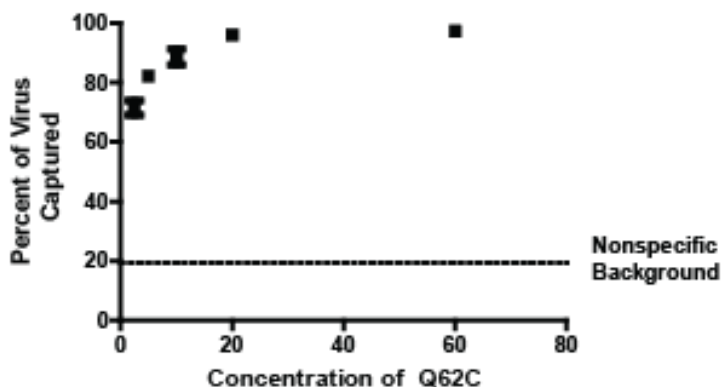


**Figure 8.** Calculated amount of virus captured using increasing concentrations of Q62C pNIPAAm. Percent of virus captured is calculated as the amount in pellet divided by the total in the supernatant and pellet. 97% virus was captured at 60 nM of Q62C pNIPAAm.

concentration. Nonspecific virus separation was determined using an equivalent amount of SA-pNIPAAm without the Q62C, and we observed ca. 20% of the virus separation, which might be caused by the non-specific interaction with mNPs and/or SA-pNIPAAm.<sup>40</sup> However, any nonspecific HIV virion separation did not impact the overall assay as the virion detection via PCR is very specific.

### HIV enrichment.

A potential approach for improving the assay detection limit is to concentrate the target analyte prior to detection. For example, utilizing 1 ml specimen with 30 copies/ml viral load provides 10-fold more RNA for detection when compared to 100  $\mu$ l specimen. Therefore, efficiently concentrating virions from larger specimen volume leads to higher downstream assay signal and the resulting assay might exhibit lower limit of detection (LOD), which can improve the assay sensitivity. To demonstrate the reagent's capability for enrichment, we applied the reagent system for concentrating 100 HIV virions/ml from

a 1000  $\mu\text{L}$  specimen. The enrichment experiments utilized pNIPAAm-SA at 31  $\mu\text{g}/\text{mL}$ , mNPs 0.5  $\text{mg}/\text{mL}$ , and biotinylated Q62C 60 nM. The magnetic separation procedure is identical to the aforementioned HIV separation. The enrichment results are summarized in Figure 9. Compared to the non-concentrated sample, 100  $\mu\text{L}$  of 100 virions/ml, the viral load of the concentrated sample increased from 1 to 15-fold when the sample volume increased from 100 to 1000  $\mu\text{L}$ . The 1000  $\mu\text{L}$  sample have a larger fold increase than 10-fold because the reagents are causing a boost in the RT-PCR signal above what should be possible. Thus, these results still need to be repeated. However, the trend is still promising when the sample volume was increased from 100 to 500  $\mu\text{L}$ , the viral load was enriched 3.5-fold. We expect this technique can be applied to concentrate larger initial sample volumes to smaller final volumes, allowing for even greater concentration factors. This technique could be useful in increasing the limit of detection

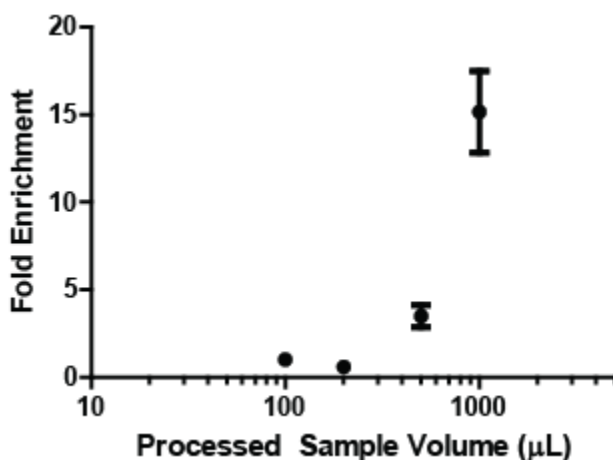


Figure 9. Q62C PNIPAAm enriches total virus at least 15 fold using increased sample volume. Pulldown assays were performed with increasing volumes of virus. Processed samples were resuspended in 100  $\mu\text{L}$  volume to achieve final viral load concentration. Fold enrichment of virus was calculated over virus in unprocessed 100  $\mu\text{L}$  volume.

of diagnostic systems limited by low sample volume when larger sample volumes are available. Future work is planned to test the performance of this system with a rapid diagnostic test.

#### 4.D. Conclusion

We have demonstrated a temperature-responsive binary reagent system that concentrates HIV using a bacterially expressed lectin, CVN. Compared to antibodies such as IgG, CVN exhibits similar binding affinity, higher stability, and low cost of production, which would be amenable for use in resource-limited settings. In order to retain the binding affinity, the binary reagent system utilized CVN mutant Q62C. The binary reagent system with biotinylated Q62C demonstrated HIV separation with 97% separation efficiency. The reagent was also able to concentrate HIV virions 3.5-fold from a 500  $\mu$ L solution, with potential for greater fold concentrations from increased volume. The reagent system is also amenable for adaptation for point-of-care, due to its simplicity and speed in comparison to existing magnetic nanoparticle separation technologies. Overall, the binary reagent system with Q62C provides enrichment of HIV and could be used with a rapid diagnostic test to increase the sensitivity when larger sample volumes are available.



## 5. References

- (1) Da Motta, L. R., Vanni, A. C., Kato, S. K., Borges, L. G. D. A., Sperhacker, R. D., Ribeiro, R. M. M., Inocêncio, L. A. (2013) Evaluation of five simple rapid HIV assays for potential use in the Brazilian national HIV testing algorithm. *J. Virol. Methods* 194, 132–137.
- (2) UNAIDS. *Global Report: UNAIDS Report on the Global AIDS Epidemic*; (2012).
- (3) Bennett, D., Bertagnolio, S., Sutherland, D., Gilks, C. (2008) The World Health Organization's global strategy for prevention and assessment of HIV drug resistance *Antivir. Ther.* 13 Suppl 2, 1–13.
- (4) World Health Organization. *Rapid advice: Antiretroviral therapy for HIV Infection in Adults and Adolescents*; (2009).
- (5) Calmy, A., Ford, N., Hirschel, B. (2007) HIV viral load monitoring in resource-limited regions: optional or necessary? *Clin. Infect.* 44.
- (6) Orrell, C., Harling, G., Lawn, S. D., Kaplan, R., McNally, M., Bekker, L.-G., Wood, R. (2007) Conservation of first-line antiretroviral treatment regimen where therapeutic options are limited. *Antivir. Ther.* 12, 83–88.
- (7) Ferradini, L., Jeannin, A., Pinoges, L., Izopet, J., Odhiambo, D., Mankhambo, L., Karungi, G., Szumilin, E., Balandine, S., Fedida, G., Carrieri, M. P., Spire, B., Ford, N., Tassie, J.-M., Guerin, P. J., Brasher, C. (2006) Scaling up of highly active antiretroviral therapy in a rural district of Malawi: an effectiveness assessment. *Lancet* 367, 1335–1342.
- (8) Mackie, N. E., Phillips, A. N., Kaye, S., Booth, C., Geretti, A.-M. (2010) Antiretroviral drug resistance in HIV-1-infected patients with low-level viremia. *J. Infect. Dis.* 201, 1303–1307.
- (9) Santoro, M. M., Fabeni, L., Armenia, D., Alteri, C., Di Pinto, D., Forbici, F., Bertoli, A., Di Carlo, D., Gori, C., Carta, S., Fedele, V., D'Arrigo, R., Berno, G., Ammassari, A., Pinnetti, C., Nicastri, E., Latini, A., Tommasi, C., Boumis, E., Petrosillo, N., D'Offizi, G., Andreoni, M., Ceccherini-Silberstein, F., Antinori, A., Perno, C. F. (2014) Reliability and Clinical Relevance of the HIV-1 Drug-Resistance Test in Patients with Low Viremia Levels. *Clin. Infect. Dis.*
- (10) Parpia, Z. a, Elghanian, R., Nabatiyan, A., Hardie, D. R., Kelso, D. M. (2010) p24 antigen rapid test for diagnosis of acute pediatric HIV infection. *J. Acquir. Immune Defic. Syndr.* 55, 413–419.

- (11) Mashayekhi, F., Chiu, R. Y. T., Le, A. M., Chao, F. C., Wu, B. M., Kamei, D. T. (2010) Enhancing the lateral-flow immunoassay for viral detection using an aqueous two-phase micellar system *Anal. Bioanal. Chem.* 398, 2955–2961.
- (12) Jue, E., Yamanishi, C. D., Chiu, R. Y. T., Wu, B. M., Kamei, D. T. (2014) Using an aqueous two-phase polymer-salt system to rapidly concentrate viruses for improving the detection limit of the lateral-flow immunoassay *Biotechnol. Bioeng.* 111, 2499–2507.
- (13) Chiu, R. Y. T., Jue, E., Yip, A. T., Berg, A. R., Wang, S. J., Kivnick, A. R., Nguyen, P. T., Kamei, D. T. (2014) Simultaneous concentration and detection of biomarkers on paper. *Lab Chip* 14, 3021–3028.
- (14) Corchero, J. L., Villaverde, A. (2009) Biomedical applications of distally controlled magnetic nanoparticles *Trends Biotechnol.* 27, 468–476.
- (15) Lai, J. J., Hoffman, J. M., Ebara, M., Hoffman, A. S., Estournès, C., Wattiaux, A., Stayton, P. S. (2007) Dual magnetic-/temperature-responsive nanoparticles for microfluidic separations and assays. *Langmuir* 23, 7385–7391.
- (16) Lai, J. J., Nelson, K. E., Nash, M. a, Hoffman, A. S., Yager, P., Stayton, P. S. (2009) Dynamic bioprocessing and microfluidic transport control with smart magnetic nanoparticles in laminar-flow devices. *Lab Chip* 9, 1997–2002.
- (17) Pelton, R. (2010) Poly(N-isopropylacrylamide) (PNIPAM) is never hydrophobic *J. Colloid Interface Sci.* 348, 673–674.
- (18) Nash, M. a, Yager, P., Hoffman, A. S., Stayton, P. S. (2010) Mixed stimuli-responsive magnetic and gold nanoparticle system for rapid purification, enrichment, and detection of biomarkers. *Bioconjug. Chem.* 21, 2197–2204.
- (19) Nash, M. a, Waitumbi, J. N., Hoffman, A. S., Yager, P., Stayton, P. S. (2012) Multiplexed enrichment and detection of malarial biomarkers using a stimuli-responsive iron oxide and gold nanoparticle reagent system. *ACS Nano* 6, 6776–6785.
- (20) Bewley, C. A., Otero-Quintero, S. (2001) The potent anti-HIV protein cyanovirin-N contains two novel carbohydrate binding sites that selectively bind to Man(8) D1D3 and Man(9) with nanomolar affinity: implications for binding to the HIV envelope protein gp120. *J. Am. Chem. Soc.* 123, 3892–3902.
- (21) Boyd, M. R., Gustafson, K. R., McMahon, J. B., Shoemaker, R. H., O’Keefe, B. R., Mori, T., Gulakowski, R. J., Wu, L., Rivera, M. I., Laurencot, C. M., Currens, M. J., Cardellina, J. H., Buckheit, R. W., Nara, P. L., Pannell, L. K., Sowder, R. C., Henderson, L. E. (1997) Discovery of cyanovirin-N, a novel human immunodeficiency virus-inactivating protein that binds viral surface envelope

- glycoprotein gp120: potential applications to microbicide development. *Antimicrob. Agents Chemother.* 41, 1521–1530.
- (22) O’Keefe, B. R., Shenoy, S. R., Xie, D., Zhang, W., Muschik, J. M., Currens, M. J., Chaiken, I., Boyd, M. R. (2000) Analysis of the interaction between the HIV-inactivating protein cyanovirin-N and soluble forms of the envelope glycoproteins gp120 and gp41. *Mol. Pharmacol.* 58, 982–992.
- (23) Xiong, S., Fan, J., Kitazato, K. (2010) The antiviral protein cyanovirin-N: the current state of its production and applications. *Appl. Microbiol. Biotechnol.* 86, 805–812.
- (24) Gao, X., Chen, W., Guo, C., Qian, C., Liu, G., Ge, F., Huang, Y., Kitazato, K., Wang, Y., Xiong, S. (2010) Soluble cytoplasmic expression, rapid purification, and characterization of cyanovirin-N as a His-SUMO fusion. *Appl. Microbiol. Biotechnol.* 85, 1051–1060.
- (25) Colleluori, D. M., Tien, D., Kang, F., Pagliei, T., Kuss, R., McCormick, T., Watson, K., McFadden, K., Chaiken, I., Buckheit, R. W., Romano, J. W. (2005) Expression, purification, and characterization of recombinant cyanovirin-N for vaginal anti-HIV microbicide development. *Protein Expr. Purif.* 39, 229–236.
- (26) Mori, T., Gustafson, K. R., Pannell, L. K., Shoemaker, R. H., Wu, L., McMahon, J. B., Boyd, M. R. (1998) Recombinant production of cyanovirin-N, a potent human immunodeficiency virus-inactivating protein derived from a cultured cyanobacterium. *Protein Expr. Purif.* 12, 151–158.
- (27) Schild, H. (1992) Poly (N-isopropylacrylamide): experiment, theory and application *Prog. Polym. Sci* 17, 163–249.
- (28) Tajima, N., Takai, M., Ishihara, K. (2011) Significance of antibody orientation unraveled: Well-oriented antibodies recorded high binding affinity *Anal. Chem.* 83, 1969–1976.
- (29) Fromme, R., Katiliene, Z., Giomarelli, B., Bogani, F., Mc Mahon, J., Mori, T., Fromme, P., Ghirlanda, G. (2007) A monovalent mutant of cyanovirin-N provides insight into the role of multiple interactions with gp120 for antiviral activity. *Biochemistry* 46, 9199–9207.
- (30) Liu, Y., Carroll, J. R., Holt, L. a, McMahon, J., Giomarelli, B., Ghirlanda, G. (2009) Multivalent interactions with gp120 are required for the anti-HIV activity of Cyanovirin. *Biopolymers* 92, 194–200.
- (31) Bewley, C. a, Gustafson, K. R., Boyd, M. R., Covell, D. G., Bax, a, Clore, G. M., Gronenborn, a M. (1998) Solution structure of cyanovirin-N, a potent HIV-inactivating protein. *Nat. Struct. Biol.* 5, 571–578.

- (32) Zappe, H., Snell, M. E., Bossard, M. J. (2008) PEGylation of cyanovirin-N, an entry inhibitor of HIV. *Adv. Drug Deliv. Rev.* 60, 79–87.
- (33) Gustafson, K. R., Sowder, R. C., Henderson, L. E., Cardellina, J. H., McMahon, J. B., Rajamani, U., Pannell, L. K., Boyd, M. R. (1997) Isolation, primary sequence determination, and disulfide bond structure of cyanovirin-N, an anti-HIV (human immunodeficiency virus) protein from the cyanobacterium *Nostoc ellipsosporum*. *Biochem. Biophys. Res. Commun.* 238, 223–228.
- (34) Malakhov, M. P., Mattern, M. R., Malakhova, O. a, Drinker, M., Weeks, S. D., Butt, T. R. (2004) SUMO fusions and SUMO-specific protease for efficient expression and purification of proteins. *J. Struct. Funct. Genomics* 5, 75–86.
- (35) Butt, T. R., Edavettal, S. C., Hall, J. P., Mattern, M. R. (2005) SUMO fusion technology for difficult-to-express proteins. *Protein Expr. Purif.* 43, 1–9.
- (36) Convertine, A. J., Benoit, D. S. W., Duvall, C. L., Hoffman, A. S., Stayton, P. S. (2009) Development of a novel endosomolytic diblock copolymer for siRNA delivery *J. Control. Release* 133, 221–229.
- (37) Hoffman, J. M., Ebara, M., Lai, J. J., Hoffman, A. S., Folch, A., Stayton, P. S. (2010) A helical flow, circular microreactor for separating and enriching “smart” polymer-antibody capture reagents. *Lab Chip* 10, 3130–3138.
- (38) Kada, G., Kaiser, K., Falk, H., Gruber, H. J. (1999) Rapid estimation of avidin and streptavidin by fluorescence quenching or fluorescence polarization. *Biochim. Biophys. Acta* 1427, 44–48.
- (39) WalkerPeach, C. R., Winkler, M., DuBois, D. B., Pasloske, B. L. (1999) Ribonuclease-resistant RNA controls (Armored RNA) for reverse transcription-PCR, branched DNA, and genotyping assays for hepatitis C virus. *Clin. Chem.* 45, 2079–2085.
- (40) Cheng, X., Canavan, H. E., Graham, D. J., Castner, D. G., Ratner, B. D. (2006) Temperature dependent activity and structure of adsorbed proteins on plasma polymerized N-isopropyl acrylamide. *Biointerphases* 1, 61.

## 6. Appendix I

Cyanovirin-N DNA sequence (Glutamine highlighted)

ATGCTTGGTAAATTCTCCCAGACCTGCTACAACCTCCGCTATCCAGGGTTCCGTTCT  
GACCTCCACCTGCGAACGTACCAACGGTGGTTACAACACCTCCTCCATCGACCTG  
AACTCCGTTATCGAAAACGTTGACGGTTCCTGAAATGGCAGCCGTCCAAC TTCAT  
CGAACCTGCCGTAACACC **CAG**CTGGCTGGTTCCTCCGAACTGGCTGCTGAATGC  
AAAACCCGTGCTCAGCAGTTCGTTTTCCACCAAATCAACCTGGACGACCACATCGC  
TAACATCGACGGTACCCTGAAATACGAATAA

Q62C DNA sequence (Cysteine highlighted)

ATGCTTGGTAAATTCTCCCAGACCTGCTACAACCTCCGCTATCCAGGGTTCCGTTCT  
GACCTCCACCTGCGAACGTACCAACGGTGGTTACAACACCTCCTCCATCGACCTG  
AACTCCGTTATCGAAAACGTTGACGGTTCCTGAAATGGCAGCCGTCCAAC TTCAT  
CGAACCTGCCGTAACACC **TGC**CTGGCTGGTTCCTCCGAACTGGCTGCTGAATGC  
AAAACCCGTGCTCAGCAGTTCGTTTTCCACCAAATCAACCTGGACGACCACATCGC  
TAACATCGACGGTACCCTGAAATACGAATAA

Cyanovirin-N Amino Acid Sequence (Glutamine highlighted)

MLGKFSQTCY NSAIQGSVLT STCERTNGGY NTSSIDLNSV IENVDGSLKW  
QPSNFIETCR NT**Q**LAGSSEL AAECKTRAQQ FVSTKINLDD HIANIDGTLK YE

Q62C Protein Amino Acid Sequence (Cysteine highlighted)

MLGKFSQTCY NSAIQGSVLT STCERTNGGY NTSSIDLNSV IENVDGSLKW  
QPSNFIETCR NT**C**LAGSSEL AAECKTRAQQ FVSTKINLDD HIANIDGTLK YE